

NATURAL CONVECTION HEAT TRANSFER WITHIN OCTAGONAL ENCLOSURE

G. Saha

*Department of Mathematics, University of Dhaka
Postal Code 1000, Dhaka, Bangladesh, rana_math06@yahoo.com*

*S. Saha**

*Department of Mechanical Engineering, The University of Melbourne
Postal Code 3010, Victoria, Australia, sumonmebuet@gmail.com*

M.N. Hasan

*Department of Mechanical Engineering, Saga University
Postal Code 840-8502, Saga, Japan, nasim@me.buet.ac.bd*

Md.Q. Islam

*Department of Mechanical Engineering, Bangladesh University of Engineering and Technology
Postal Code 1000, Dhaka, Bangladesh, quamrul@me.buet.ac.bd*

*Corresponding Author

(Received: February 2, 2009 – Accepted in Revised Form: July 2, 2009)

Abstract The problem of steady, laminar and incompressible natural convection flow in an octagonal enclosure was studied. In this investigation, two horizontal walls were maintained at a constant high temperature, two vertical walls were kept at a constant low temperature and all inclined walls were considered adiabatic. The enclosure was assumed to be filled with a Boussinesq fluid. The study includes computations for different Prandtl numbers Pr such as 0.71, 7, 20 and 50 whereas the Rayleigh number Ra was varied from 10^3 to 10^6 . The pressure-velocity form of Navier-Stokes equations and energy equation were used to represent the mass, momentum and energy conservations of the fluid medium in the enclosure. The governing equations and boundary conditions were converted to dimensionless form and solved numerically by penalty finite element method with discretization by triangular mesh elements. Flow and heat transfer characteristics were presented in terms of streamlines, isotherms and average Nusselt number Nu . Results showed that the effect of Ra on the convection heat transfer phenomenon inside the enclosure was significant for all values of Pr studied (0.71-50). It was also found that, Pr influence natural convection inside the enclosure at high Ra ($Ra > 10^4$).

Keywords Natural Convection, Penalty Finite Element, Nusselt Number, Octagonal Enclosure, Rayleigh Number

چکیده جابه‌جایی طبیعی جریان پایدار، آرام و تراکم‌ناپذیر درون یک فضای هشت‌وجهی مطالعه شده است. در این بررسی دو دیواره افقی در یک دمای بالا و دو دیواره عمودی در دمای پایین ثابت نگه داشته شد و تمام دیواره‌های مورب آدیاباتیک در نظر گرفته شد. همچنین فرض شد که فضای هشت‌وجهی با سیال پر شده باشد. این بررسی شامل محاسبات مربوط به اعداد پرنتل متفاوت است؛ مانند: 0.71، 7، 20 و 50 را در حالی که عدد رایلی از 10^3 تا 10^6 متغیر بود. برای بیان معادلات جرم، مومنتم و انرژی سیال در فضای مورد نظر از فرم فشار-سرعت معادلات ناویر-استوکس و معادله انرژی استفاده شد. معادلات به دست آمد و شرایط مرزی بدون بعد شد و با روش تفاضل محدود پنالتی و جداسازی المان‌های مش مثلثی حل شد. خصوصیات انتقال حرارت و جریان به صورت خطوط جریان، ایزوترم‌ها و عدد ناسلت متوسط نشان داده شد. نتایج نشان داد که تأثیر عدد رایلی روی انتقال حرارت جابه‌جایی در فضای مورد نظر برای همه مقادیر عدد پرنتل (0.71-50) چشمگیر است. همچنین از نتایج استنباط شد که عدد پرنتل در عدد رایلی بالا ($Ra > 10^4$) روی جابه‌جایی طبیعی در فضای هشت‌وجهی تأثیر می‌گذارد.

1. INTRODUCTION

Analysis of natural convection finds applications in

thermal insulation, cooling of electronic devices, solar energy instruments, nuclear reactors, heat-recovery systems, room ventilation, crystal growth

in liquids and tower type architectural structure, etc. The fluid flow and heat transfer behavior of such systems can be predicted by mass, momentum and energy conservation equations considering appropriate boundary conditions.

Actual enclosures in practice are often found to have different shapes rather than rectangular ones. Some examples of non-rectangular channels include various channels of constructions, panels of electronic equipment and solar energy collectors, etc. Several geometrical configurations, more or less complex, have been examined under theoretical, numerical or experimental approaches. Heat transfer experiments in triangular enclosures were first reported by Flack, et al [1]. Effect of non-uniform heat flux on convection heat transfer in trapezoidal channel was experimentally studied by Remley, et al [2]. Kumar [3] experimentally investigated natural convective heat transfer in trapezoidal enclosure. He focused on the performance of a box type solar cooker and evaluated the natural convective heat transfer coefficient. Natural convection in tilted parallelepiped cavities for large Rayleigh numbers was studied numerically and experimentally by Baïri, et al [4]. The majority of researches involved in convection study are restricted to the cases of simple geometries like rectangular, square, cylindrical and spherical cavities. However, the configurations of actual containers occurring in practice are often far from simple ones. Heat and mass transfer by free convection in a trapezoidal enclosure with hot lower wall and cold side walls was studied by Boussaid, et al [5]. In that research work, momentum, energy and mass equations were solved by finite volume method and the influences of the geometrical parameters were observed. Kuyper, et al [6] investigated laminar natural convection flow in trapezoidal enclosures to study the influence of the inclination angle on the flow and also the dependence of the average Nusselt number on the Rayleigh number. Iyican, et al [7], McQuain, et al [8], Van der Eyden, et al [9], Reynolds, et al [10], Papanicolaou, et al [11] and several other researchers have several attempts to understand the basic heat transfer and fluid flow characteristics inside a trapezoidal cavity.

To the best of the author's knowledge, no attention has been paid to the problem of natural convection of flow and heat transfer within an

octagonal enclosure whose inclined walls are considered adiabatic with other vertical and horizontal walls maintained at constant high and low temperature, respectively. The objective of the present study is to examine the effect of Rayleigh and Prandtl numbers within an octagonal enclosure for the above mentioned boundary conditions. The results are presented in terms of parametric presentations of streamline and isotherm plots inside the enclosure and the variation of the average Nusselt number at the heated surfaces with the change of governing parameters are also discussed briefly.

2. PROBLEM FORMULATION

The present paper considers the problem of natural convection in an octagonal enclosure where different working fluids have been considered for simulation. The length of each sides of the enclosure is assumed to be equal to L . The physical model considered here is shown in Figure 1 along with the important geometric parameters and boundary conditions. The vertical left and right walls are kept at fixed high temperature, T_h whereas, the top and bottom horizontal walls are at constant low temperature, T_c ($T_c < T_h$). In the present

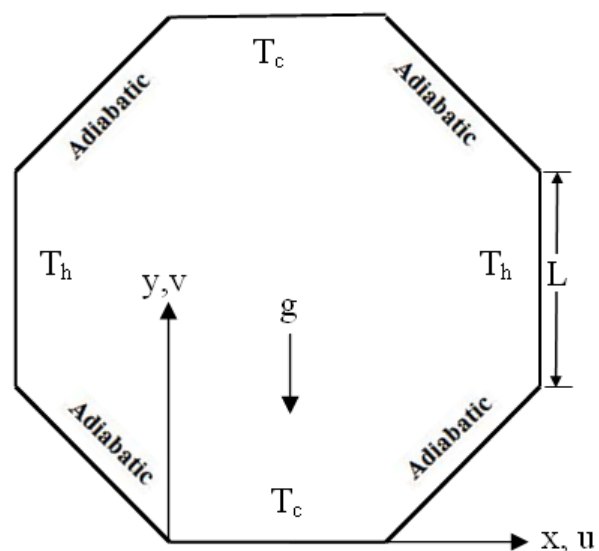


Figure 1. Schematic diagram of the physical system.

work, a steady two-dimensional laminar flow of incompressible fluid is considered with negligible viscous dissipation effect. For the treatment of the buoyancy term in the momentum equation, Boussinesq approximation is adopted to account for the variations of temperature as a function of density as well as to couple the temperature field with the flow field. With the above mentioned assumptions, the governing equations for steady natural convection flow using conservation of mass, momentum and energy can be expressed in the following dimensionless form as follow:

$$\frac{\partial U}{\partial X} + \frac{\partial V}{\partial Y} = 0 \quad (1)$$

$$U \frac{\partial U}{\partial X} + V \frac{\partial U}{\partial Y} = -\frac{\partial P}{\partial X} + \text{Pr} \left(\frac{\partial^2 U}{\partial X^2} + \frac{\partial^2 U}{\partial Y^2} \right) \quad (2)$$

$$U \frac{\partial V}{\partial X} + V \frac{\partial V}{\partial Y} = -\frac{\partial P}{\partial Y} + \text{Pr} \left(\frac{\partial^2 V}{\partial X^2} + \frac{\partial^2 V}{\partial Y^2} \right) + \text{Ra Pr } \Theta \quad (3)$$

$$U \frac{\partial \Theta}{\partial X} + V \frac{\partial \Theta}{\partial Y} = \left(\frac{\partial^2 \Theta}{\partial X^2} + \frac{\partial^2 \Theta}{\partial Y^2} \right) \quad (4)$$

Where, X and Y are the non-dimensional coordinates along the horizontal and vertical directions, respectively, U and V are the non-dimensional velocity components in the X and Y directions, respectively, Θ is the non-dimensional temperature and P is the non-dimensional pressure. The non-dimensional numbers appeared in the governing equations, Ra and Pr are the Rayleigh number and Prandtl number respectively and are defined as follows:

$$\text{Ra} = \frac{g\beta\Delta T L^3}{\alpha\nu} \quad \text{and} \quad \text{Pr} = \frac{\nu}{\alpha} \quad (5)$$

The dimensionless parameters in the previous equations are defined as follow:

$$X = \frac{x}{L}, Y = \frac{y}{L}, U = \frac{uL}{\nu}, V = \frac{vL}{\nu}, \quad (6)$$

$$P = \frac{pL^2}{\rho\nu^2}, \Theta = \frac{T - T_c}{\Delta T}, \Delta T = T_h - T_c$$

Where, ρ , β , ν , α and g are the fluid density, coefficient of volumetric expansion, kinematic viscosity, thermal diffusivity and gravitational acceleration, respectively. Among others x , y are Cartesian coordinates while p and T denote pressure and temperature, respectively.

The boundary conditions for the present problem are specified as follow:

- For horizontal walls: $U = V = \Theta = 0$
- For vertical walls: $U = V = 0, \Theta = 1$
- For inclined walls: $U = V = \frac{\partial \Theta}{\partial n} = 0$, where n is the outward normal dimensionless length.

The sum of the average Nusselt number at the hot walls of the enclosure may be expressed as:

$$\text{Nu} = -\int_0^1 \left. \frac{\partial \Theta}{\partial X} \right|_{\text{left}} dY + \int_0^1 \left. \frac{\partial \Theta}{\partial X} \right|_{\text{right}} dY \quad (7)$$

In the present study, numerical simulations are carried out for parametric variation of Rayleigh numbers, Ra from 10^3 to 10^6 with Prandtl number of 0.71, 7, 20 and 50, respectively.

3. FINITE ELEMENT FORMULATION

The continuity Equation 1 can be used as a constraint due to the mass conservation and it may be used to obtain the pressure distribution. In order to solve Equations 2-4, Penalty finite element method [12] has been used, where the pressure P is eliminated by Penalty parameter γ and the incompressibility criteria is given by Equation 1 which results in:

$$P = -\gamma \left(\frac{\partial U}{\partial X} + \frac{\partial V}{\partial Y} \right) \quad (8)$$

The continuity Equation 1 is automatically satisfied for large values of γ . Using Equation 8, the momentum Equations 2 and 3 reduce to:

$$U \frac{\partial U}{\partial X} + V \frac{\partial U}{\partial Y} = \gamma \frac{\partial}{\partial X} \left(\frac{\partial U}{\partial X} + \frac{\partial V}{\partial Y} \right) + \text{Pr} \left(\frac{\partial^2 U}{\partial X^2} + \frac{\partial^2 U}{\partial Y^2} \right) \quad (9)$$

$$U \frac{\partial V}{\partial X} + V \frac{\partial U}{\partial Y} = \gamma \frac{\partial}{\partial Y} \left(\frac{\partial U}{\partial X} + \frac{\partial V}{\partial Y} \right) + \text{Pr} \left(\frac{\partial^2 V}{\partial X^2} + \frac{\partial^2 V}{\partial Y^2} \right) + \text{RaPr}\Theta \quad (10)$$

Expanding the velocity components (U,V) and temperature (Θ) using basis set $\{N_k\}_{k=1}^N$ we get:

$$U \approx \sum_{k=1}^N U_k N_k, V \approx \sum_{k=1}^N V_k N_k \text{ and } \Theta \approx \sum_{k=1}^N \Theta_k N_k \quad (11)$$

Then Galerkin finite element method yields the following nonlinear residual equations for Equations 9-11, respectively at nodes of internal domain A.

$$\begin{aligned} R_i^{(1)} &= \sum_{k=1}^N U_k \int_{\Omega} \\ &\left[\left(\sum_{k=1}^N U_k N_k \right) \frac{\partial N_k}{\partial X} + \left(\sum_{k=1}^N V_k N_k \right) \frac{\partial N_k}{\partial Y} \right] N_i dXdY + \\ &\gamma \left[\sum_{k=1}^N U_k \int_{\Omega} \left(\frac{\partial N_i}{\partial X} \frac{\partial N_k}{\partial X} \right) dXdY + \sum_{k=1}^N V_k \int_{\Omega} \left(\frac{\partial N_i}{\partial Y} \frac{\partial N_k}{\partial Y} \right) dXdY \right] + \\ &\text{Pr} \sum_{k=1}^N U_k \int_{\Omega} \left(\frac{\partial N_i}{\partial X} \frac{\partial N_k}{\partial X} + \frac{\partial N_i}{\partial Y} \frac{\partial N_k}{\partial Y} \right) dXdY \end{aligned} \quad (12)$$

$$\begin{aligned} R_i^{(2)} &= \sum_{k=1}^N V_k \int_{\Omega} \left[\left(\sum_{k=1}^N U_k N_k \right) \frac{\partial N_k}{\partial X} + \left(\sum_{k=1}^N V_k N_k \right) \frac{\partial N_k}{\partial Y} \right] N_i dXdY \\ &+ \gamma \left[\sum_{k=1}^N U_k \int_{\Omega} \left(\frac{\partial N_i}{\partial X} \frac{\partial N_k}{\partial X} \right) dXdY + \sum_{k=1}^N V_k \int_{\Omega} \left(\frac{\partial N_i}{\partial Y} \frac{\partial N_k}{\partial Y} \right) dXdY \right] \\ &+ \text{Pr} \sum_{k=1}^N V_k \int_{\Omega} \left(\frac{\partial N_i}{\partial X} \frac{\partial N_k}{\partial X} + \frac{\partial N_i}{\partial Y} \frac{\partial N_k}{\partial Y} \right) dXdY \\ &\text{RaPr} \int_{\Omega} \left(\sum_{k=1}^N \Theta_k N_k \right) N_i dXdY \end{aligned} \quad (13)$$

$$\begin{aligned} R_i^{(3)} &= \sum_{k=1}^N \Theta_k \int_{\Omega} \left[\left(\sum_{k=1}^N U_k N_k \right) \frac{\partial N_k}{\partial X} + \left(\sum_{k=1}^N V_k N_k \right) \frac{\partial N_k}{\partial Y} \right] dXdY \\ &+ \sum_{k=1}^N \Theta_k \int_{\Omega} \left(\frac{\partial N_i}{\partial X} \frac{\partial N_k}{\partial X} + \frac{\partial N_i}{\partial Y} \frac{\partial N_k}{\partial Y} \right) dXdY \end{aligned} \quad (14)$$

Three point Gaussian quadratic formulas are used to evaluate the integrals in the residual equations. The nonlinear residual Equations 12-14 are solved using Newton's method to determine the coefficients of the expansions in Equation 11. Also

$$X = \sum_{k=1}^6 X_k N_k(\xi, \eta) \text{ and } Y = \sum_{k=1}^6 Y_k N_k(\xi, \eta) \quad (15)$$

Where, $N_i(\xi, \eta)$ are the local six noded triangular basis functions in ξ - η domain. The integrals in Equations 12-14 can be evaluated in ξ - η domain using the following relationships:

$$\begin{bmatrix} \frac{\partial N_i}{\partial X} \\ \frac{\partial N_i}{\partial Y} \end{bmatrix} = \frac{1}{J} \begin{bmatrix} \frac{\partial Y}{\partial \eta} & -\frac{\partial Y}{\partial \xi} \\ -\frac{\partial X}{\partial \eta} & \frac{\partial X}{\partial \xi} \end{bmatrix} \begin{bmatrix} \frac{\partial N_i}{\partial \xi} \\ \frac{\partial N_i}{\partial \eta} \end{bmatrix} \text{ and } dXdY = J d\xi d\eta \quad (16)$$

Where,

$$J = \frac{\partial(X, Y)}{\partial(\xi, \eta)} = \begin{vmatrix} \frac{\partial X}{\partial \xi} & \frac{\partial X}{\partial \eta} \\ \frac{\partial Y}{\partial \xi} & \frac{\partial Y}{\partial \eta} \end{vmatrix} \quad (17)$$

4. RESULTS AND DISCUSSIONS

The numerical procedure that has been used to solve the governing equations for the present work is Penalty finite element method. It provides smooth solutions in the interior domain including the corner regions. The non-linear parametric solution is chosen to solve the governing equations. This approach will result in substantially fast convergence assurance. A non-uniform triangular mesh arrangement is implemented in the current investigation especially, near the heated wall to capture the rapid changes in the dependent variables. Also, six noded triangular elements are considered in the present model since the six noded elements smoothly capture the non-linear variations of the field variables. All six nodes are associated with velocity as well as temperature while only the corner nodes are associated with pressure. The

relative tolerance for the error criteria is considered to be 10^{-6} . As the dependent variables vary greatly in magnitude, manual scaling of the dependent variables is used to improve numerical convergence. The manual scaling values are kept constant and selected in such a way that the magnitudes of the scaled degrees of freedom become unity.

4.1. Grid Sensitivity Check Test for the accuracy of the grid sensitivity is examined for the arrangements of five different non-uniform grid systems with the following number of elements within the octagonal enclosure: 5829, 7121, 8796, 10466 and 13658. The results are shown in Table 1. From these comparisons, it is suggested that 10466 non-uniform elements are sufficient to produce accurate results.

4.2. Code Validation Since validation of experimental data is not possible in the present case; the computational code is validated with the results obtained for natural convection flows in a trapezoidal enclosure as mentioned by Natarajan, et al [13]. Comparison of the result is shown in Figure 2 and it has been observed that the present numerical solution is almost in full agreement with the aforementioned one in terms of the isotherm plot. Therefore, it can be concluded that the current code can be used to predict the flow and thermal field for the present problem accurately. However, almost similar experimental results for square straight enclosure with discrete bottom heating obtained by Corvaro, et al [14] are compared by the present code and reported in Table 2. The agreement is found to be excellent which validates the present computations and lead us confidence for the use of the present code.

4.3. Flow and Thermal Fields The thermal and dynamical velocity field the investigated octagonal enclosure are depicted in Figure 3 for $Pr = 0.71$ air and Ra ranging from 10^3 to 10^6 . The opposite walls of the octagonal enclosure along the vertical axis are hot isothermal surfaces (T_h) while those along the horizontal axis are cooled (T_c) with the other four inclined walls at the corners are being adiabatic. Due to the density gradient of the fluid in the vicinity of the hot and cold walls, a convection current is set up that causes the hot fluid to rise up along the vertical side walls whilst,

TABLE 1. Comparison of the Results for Various Grid Dimensions at $Ra = 10^3$ and $Pr = 0.71$.

Elements	Nusselt Number, Nu
5829	2.4105
7121	2.4128
8796	2.4437
10466	2.4544
13658	2.4544

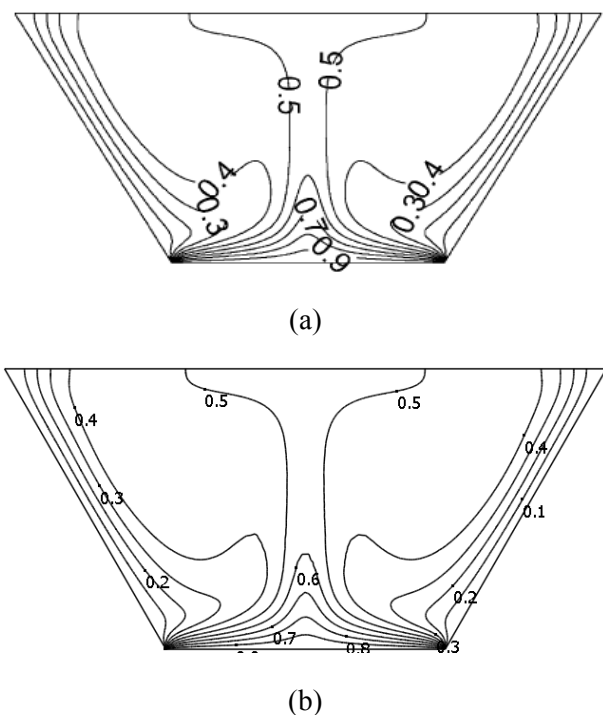


Figure 2. Comparison of the isotherm plots by Natarajan, et al [13] at $Ra = 10^3$ and $Pr = 0.71$, (a) Natarajan, et al [13] and (b) Present Code.

cold fluid comes down through the middle portion of the enclosure forming two symmetric rolls with clockwise and counter clockwise rotations. The obtained results clearly reveal dependency of the streamlines number Ra as shown in Figure 3.

Figure 3a shows the temperature and streamline distribution inside the enclosure for $Pr = 0.71$ and $Ra = 10^3$. In this case, the streamline distribution

TABLE 2. Comparison Between the Experimental and Numerical Average Nusselt Number.

Rayleigh Number, Ra	Average Nusselt Number		Error (%)
	Experimental Data Obtained by Corvaro, et al [14]	Numerical Data (Present Code)	
7.56×10^4	4.80	5.31	10.63
1.38×10^5	5.86	6.07	3.60
1.71×10^5	6.30	6.37	1.11
1.98×10^5	6.45	6.58	2.01
2.32×10^5	6.65	6.82	2.56
2.50×10^5	6.81	6.94	1.91

consists of two identical rolls inside the enclosure while the isotherms are found to be symmetric only with respect to vertical central axis. The asymmetry of isotherms with respect to the horizontal axis is due to differential convection effect experienced by the cold walls located at the top and bottom of the enclosure. Near the central core at the lower half of the enclosure, there are small gradients in temperature whereas a large stratification zone of temperature is observed at the vertical symmetric line near the top wall. The pronounced convection effect acting on the top cold wall results in densely spaced isotherms while those near the bottom cold wall are found to be flatter as shown the Figure 3a.

As Rayleigh number increases, significant change in the contour of isotherms occurs as shown in Figures 3b-3d. While $Pr = 0.71$, these Figures 3b-3d illustrate the streamlines and isotherms for $Ra = 10^4$, 10^5 and 10^6 , respectively. With the increase of Rayleigh number Ra , enhanced buoyancy strengthens the convection circulation which in turn results in significant distortion of the isotherms inside the enclosure. At high Ra , part of the flow that is deflected by the upper corner walls towards the center of the enclosure plays vital role in reshaping the streamlines and isotherms. All isotherms are pushed closer to the walls from the center of the enclosure under increasingly “Y” shaped flow. The isotherms that are almost flat near the bottom cold wall at $Ra = 10^3$, become concave at $Ra = 10^6$. At high Ra , some secondary flows are

observed near the bottom cold wall as shown in Figures 3c,d.

In the present study, it is found that effect of Prandtl number Pr on natural convection phenomena inside the octagonal enclosure for the given boundary conditions does not affect significantly for lower value of Rayleigh number ($Ra < 10^4$). For simplicity, the isotherm and streamline distribution for $Ra = 10^3, 10^4$ are not included here. This phenomenon will also be clear from the heat transfer characteristics later. The effect of Pr on convection characteristics inside the enclosure is shown in Figure 4 for $Ra = 10^6$. As Pr increases, the circulation strength also increases and the zone of stratification of the temperature at the vertical symmetric line increases. Consequently, it causes more and more compression of the isotherms towards the boundary of the enclosure. The contour of the isotherms near the bottom cold wall indicates enhanced heat transfer towards the lower half of the enclosure for high Pr number. The secondary convection current at lower part of the enclosure becomes more prominent with high Prandtl number.

4.4. Heat Transfer Characteristics The overall effects upon the heat transfer rates are depicted in Figure 5, where variation of sum of the average Nusselt number Nu of the two opposite hot walls of the octagonal enclosure, as defined by Equation 7, is shown in logarithmic scale with Rayleigh number for different Prandtl numbers.

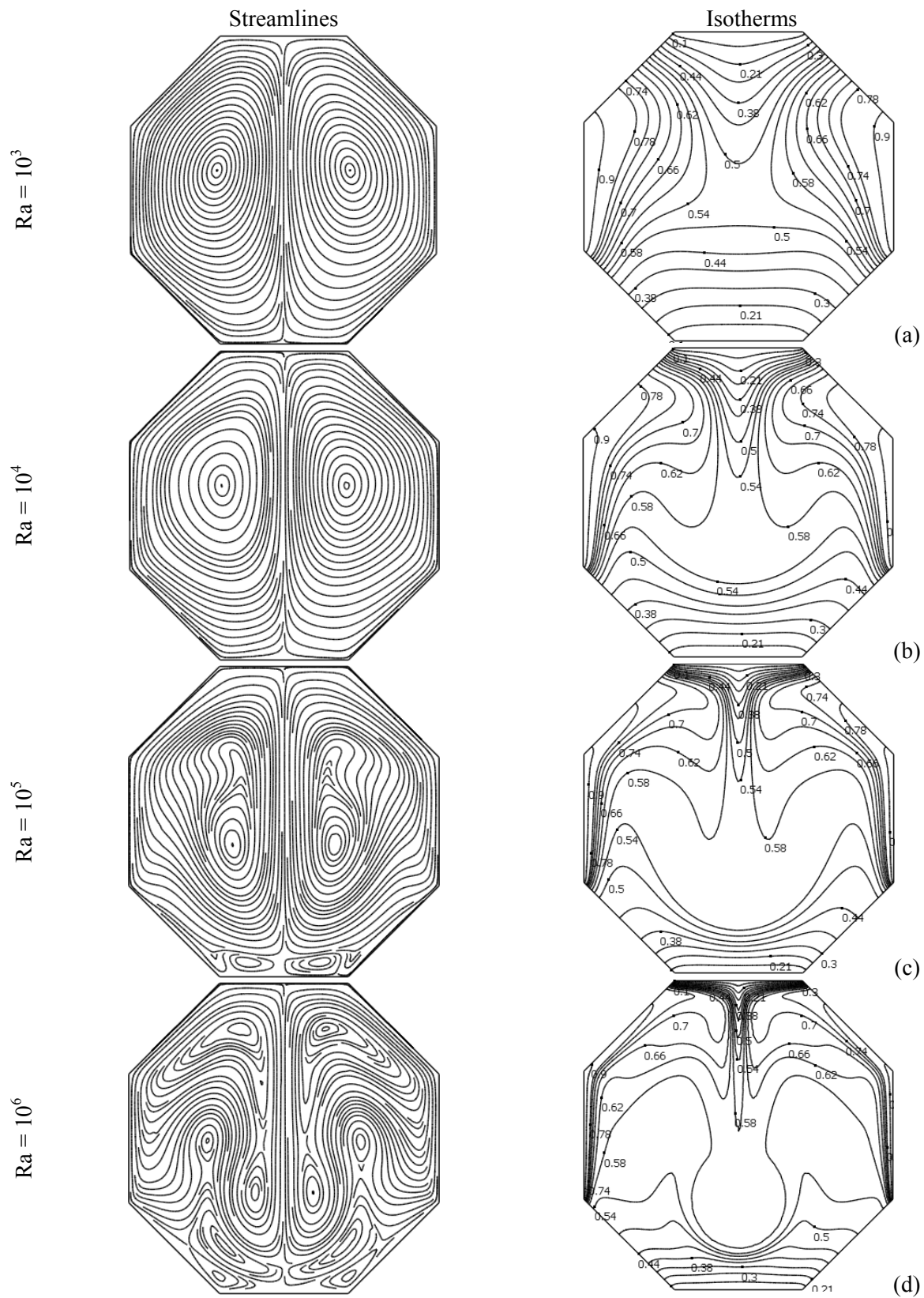


Figure 3. Distribution of streamlines and isotherms for different Ra at $Pr = 0.71$.

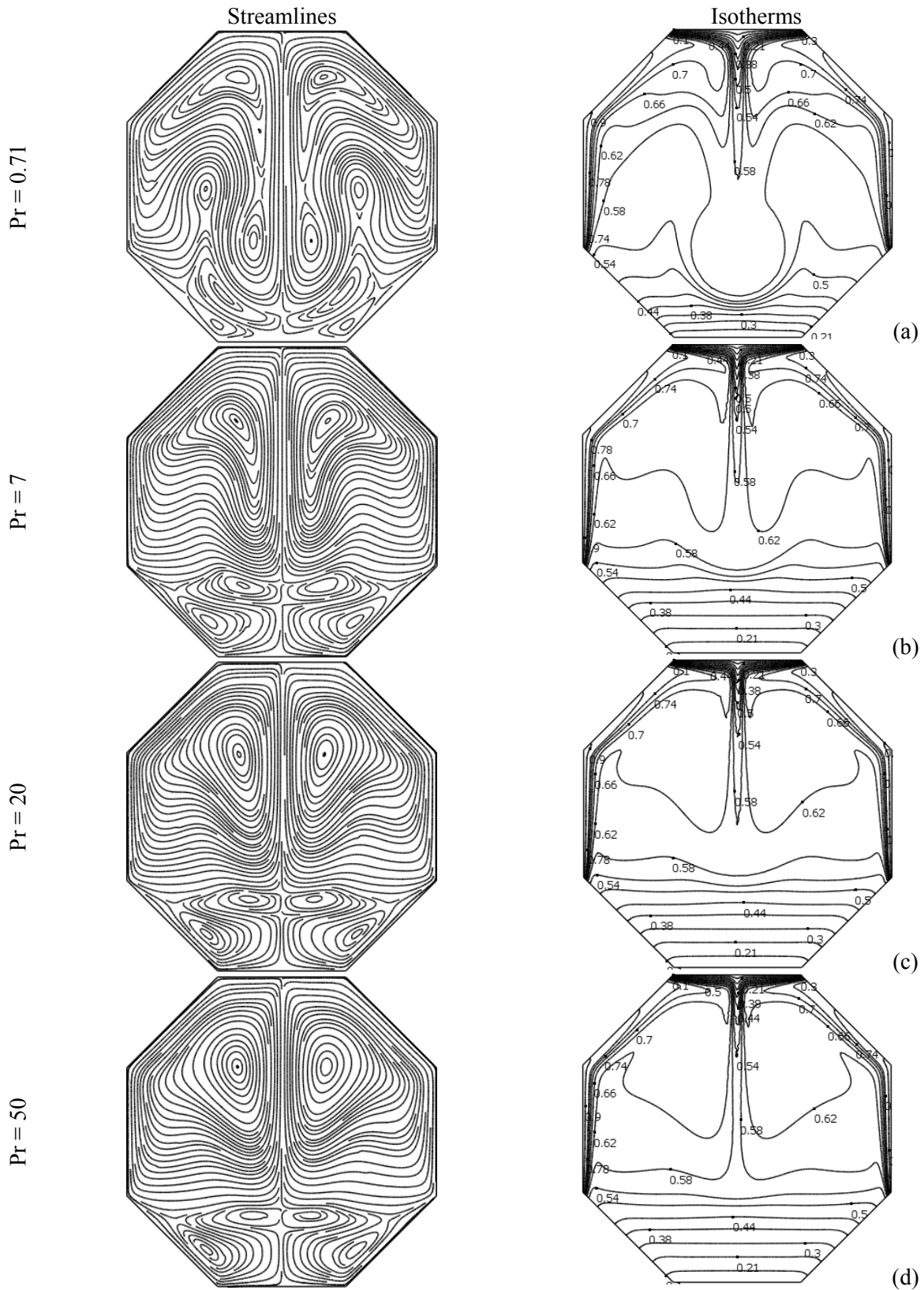


Figure 4. Distribution of streamlines and isotherms for different Pr at $Ra = 10^6$.

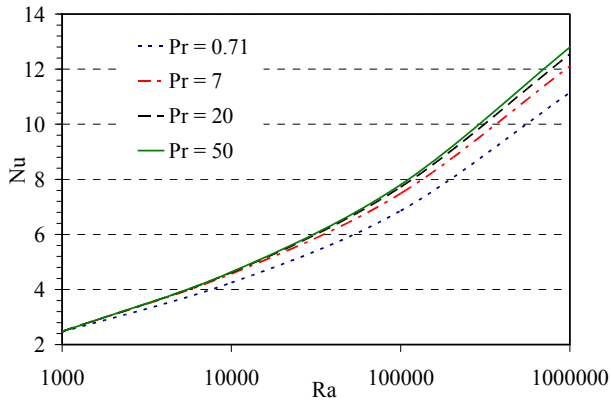


Figure 5. Average Nusselt number variation as a function of Rayleigh number for different Prandtl numbers.

It is worth to mention that for $Ra = 10^3$, the distribution of isotherms and streamlines do not alter for all values of Pr ($0.71 < Pr < 50$). Distribution of the isotherms indicates conduction dominant heat transfer at $Ra = 10^3$. From Figure 5, it is clear that for $Ra > 10^3$, average Nusselt number increases with Rayleigh number but the rate of increment is pronounced at high range of Ra ($Ra \geq 10^5$). For a particular value of Ra , heat transfer also increases as Prandtl number increases but at high range of Prandtl number, relative increase of Nu is not significant compared to Ra as shown in Figure 5.

5. CONCLUSION

Two-dimensional numerical simulation of natural convection inside an octagonal enclosure with two hot walls (side walls) and two cold walls (top and bottom walls) separated consecutively by four adiabatic walls (corner inclined walls) has been performed in the present study. From the analysis of the streamline and isotherm patterns, it is found that conduction dominant heat transfer prevails inside the enclosure up to $Ra = 10^3$. Both the Rayleigh number and Prandtl number are found to influence the convection characteristics inside the enclosure. It is interesting that at high values of Rayleigh number, the bottom cold wall undergoes progressively higher cooling effect than the top one. Not only that, some secondary circulation

occurs at the bottom half of the enclosure at high Rayleigh number due to the deflection of strong circulation caused by the corner walls. Finally, the overall heat transfer from the hot walls is found to increase with Rayleigh number and the effect is found to be amplified at higher values of Ra . Similar result is also observed for the variation of Prandtl number at higher values of Ra ($Ra > 10^4$) but its effect seems to lessen at higher values of Pr compared with Ra .

6. REFERENCES

1. Flack, R.D., Konopnicki, T.T. and Rooke, J.H., "The Measurement of Natural Convective Heat Transfer in Triangular Enclosure", *Journal of Heat Transfer, Transaction of ASME*, Vol. 102, (1980), 770-772.
2. Remley, T. J., Abdel-Khalik, S. I., Jeter, S. M., Ghiaasiaan, S. M. and Dowling, M. F., "Effect of Non-Uniform Heat Flux on Wall Friction and Convection Heat Transfer Coefficient in a Trapezoidal Channel", *International Journal of Heat and Mass Transfer*, Vol. 44, (2001), 2453-2459.
3. Kumar, S., "Natural Convective Heat Transfer in a Trapezoidal Enclosure of Box-Type Solar Cooker", *Renewable Energy*, Vol. 29, (2004), 211-222.
4. Baire, A., Laraqi, N. and Garcia de Maria, J.M., "Numerical and Experimental Study of Natural Convection in Tilted Parallelepipedic Cavities for Large Rayleigh Numbers", *Experimental Thermal and Fluid Science*, Vol. 31, (2007), 309-324.
5. Boussaid, M., Mezener, A. and Bouhadeh, M., "Free Heat and Mass Convection in a Trapezoidal Enclosure", *International Journal of Thermal Science*, Vol. 38, (1999), 363-371.
6. Kuypers, R.A. and Hoogendoorn, C.J., "Laminar Natural Convection Flow in Trapezoidal Enclosures", *Numerical Heat Transfer, Part A*, Vol. 28, (1995), 55-67.
7. Iyican, L. and Bayazitoglu, Y., "An Analytical Study of Natural Convective Heat Transfer within Trapezoidal Enclosure", *Journal of Heat Transfer, Transaction of ASME*, Vol. 102, (1980), 640-647.
8. McQuain, W.D., Ribbens, C.J., Wang, C.Y. and Watson, L.T., "Steady Viscous Flow in a Trapezoidal Cavity", *Computers and Fluids*, Vol. 23, (1994), 613-626.
9. Vander Eyden, J.T., Van der Meer, TH.H., Hanjalić, K., Biezen, E. and Bruining, J., "Double-Diffusive Natural Convection in Trapezoidal Enclosures", *International Journal of Heat and Mass Transfer*, Vol. 13, (1998), 1885-1898.
10. Reynolds, D.J., Jance, M.J., Behnia, M. and Morrison, G.L., "An Experimental and Computational Study of the Heat Loss Characteristics of a Trapezoidal Cavity Absorber", *Solar Energy*, Vol. 76, (2004), 229-234.
11. Papanicolaou, E., and Belessiotis, V., "Double-Diffusive Natural Convection in an Asymmetric Trapezoidal

- Enclosure: Unsteady Behavior in the Laminar and the Turbulent-Flow Regime”, *International Journal of Heat and Mass Transfer*, Vol. 48, (2005), 191-209.
12. Basak, T., Roy, S., and Balakrishnan, A. R., “Effects of Thermal Boundary Conditions on Natural Convection Flows within a Square Cavity”, *International Journal of Heat and Mass Transfer*, Vol. 49, (2006), 4525-4535.
 13. Natarajan, E., Basak, T. and Roy, S., “Natural Convection Flows in a Trapezoidal Enclosure with Uniform and Non-uniform Heating of Bottom Wall”, *International Journal of Heat and Mass Transfer*, Vol. 51, (2008), 747-756.
 14. Corvaro, F. and Paroncini, M., “A Numerical and Experimental Analysis on the Natural Convection Heat Transfer of a Small Heating Strip Located on the Floor of a Square Cavity”, *Applied Thermal Engineering*, Vol. 28, (2008), 25-35.